Ultrashort laser pulse filamentation from spontaneous X Wave formation in air

Daniele Faccio[1], Alessandro Averchi[1], Antonio Lotti[1], Paolo Di Trapani[1,2], Arnaud Couairon[3], Dimitris Papazoglou[4,5], Stelios Tzortzakis[5]

[1] *CNISM and Department of Physics and Mathematics, Università dell'Insubria, Via Valleggio 11, IT-22100 Como, Italy*

[2] *Department of Quantum Electronics, Vilnius University, Saulėtekio Ave. 9, bldg.3, LT-10222, Vilnius, Lithuania*

[3] *Centre de Physique Théorique, CNRS, École Polytechnique, F-91128, Palaiseau, France*

[4] *Materials Science and Technology Department, University of Crete, P.O. Box 2208, 71003, Heraklion, Greece*

[5] *Institute of Electronic Structure and Laser, Foundation for Research and Technology Hellas, P.O. Box 1527, 71110, Heraklion, Greece*

daniele.faccio@uninsubria.it

Abstract: The description of ultrashort laser pulse filamentation in condensed media as a spontaneous formation of X waves is shown to apply also to filaments generated in air. Within this framework, a simple explanation is brought for several features of the filament such as the subdiffractive propagation and the energy flux from the weakly localized tails of the X-waves to the intense core.

OCIS codes: (190.5940) Self-action effects; (320.2250) Femtosecond phenomena; (190.5890) Scattering, stimulated.

References and links

1. A. Couairon and A. Mysyrowicz, "Femtosecond filamentation in transparent media," Phys. Rep. **441**, 47-189 (2007).
2. F. Théberge, N. Aközbek , W. Liu, A. Becker, and S. L. Chin, "Tunable Ultrashort Laser Pulses Generated through Filamentation in Gases," Phys. Rev. lett. **97**, 023904 (2006)
3. A. Couairon, J. Biegert, C. P. Hauri, W. Kornelis, F. W. Helbing, U. Keller, and A. Mysyrowicz, "Self-compression of ultra-short laser pulses down to one optical cycle by filamentation," J. Mod. Opt. **53**, 75-85 (2006).
4. S. Tzortzakis, M.A. Franco, Y.B. André, A. Chiron, B. Lamouroux, B.S. Prade, and A. Mysyrowicz, "Formation of a conducting channel in air by self-guided femtosecond laser pulses," Phys. Rev. E **60**, 3505–3508 (1999)
5. A. Braun, G. Korn, X. Liu, D. Du, J. Squier, and G. Mourou, "Self-channeling of high-peak-power femtosecond laser pulses in air," Opt. Lett. **20**, 73-75 (1995)
6. M. Mlejnek, E.M. Wright, and J.V. Moloney, "Dynamic spatial replenishment of femtosecond pulses propagating in air," Opt. Lett. **23**, 382–384 (1998)
7. X.M. Zhao and J.C. Diels, "Femtosecond pulses to divert lightning," Laser Focus World **29**, 113–123 (1993)
8. S. Tzortzakis, B. Prade, M. Franco, A. Mysyrowicz, S. Hüller, and P. Mora, "Femtosecond laser-guided electric discharge in air," Phys. Rev. E **64**, 057401 (2001)
9. B. La Fontaine, D. Comtois, C.-Y. Chien, A. Desparois, F. Génin, G. Jarry, T. Johnston, J.-C. Kieffer, F. Martin, R. Mawassi, H. Pépin, F. A. M. Rizk, F. Vidal, C. Potvin, P. Couture and H. P. Mercure, "Guiding large-scale spark discharges with ultrashort pulse laser filaments," J. Appl. Phys. **88**, 610–615 (2000)
10. C. D'Amico, A. Houard, M. Franco, B. Prade, A. Mysyrowicz, A. Couairon, and V.T. Tikhonchuk, "Conical forward THz emission from femtosecond-laser-beam filamentation in air," Phys. Rev. Lett. **98** 235002 (2007)
11. G. Méchain, C.D'Amico, Y.-B. André, S. Tzortzakis, M. Franco, B. Prade, A. Mysyrowicz, A. Couairon, E. Salmon, R. Sauerbrey, "Long-range self-channeling of infrared laser pulses in air: a new propagation regime without ionization," Appl. Phys. B **79**, 379–382 (2004)

#89996 - $15.00 USD Received 21 Nov 2007; revised 14 Jan 2008; accepted 16 Jan 2008; published 22 Jan 2008

12. S. Eisenmann, A. Pukhov, and A. Zigler, "Fine Structure of a Laser-Plasma Filament in Air," Phys. Rev. Lett. **98**, 155002 (2007)
13. M. Kolesik, E.M. Wright and J.V. Moloney, "Dynamic Nonlinear X Waves for Femtosecond Pulse Propagation in Water," Phys. Rev. Lett. **92**, 253901 (2004).
14. D. Faccio, M. A. Porras, A. Dubietis, F. Bragheri, A. Couairon, and P. Di Trapani, "Conical Emission, Pulse Splitting, and X-Wave Parametric Amplification in Nonlinear Dynamics of Ultrashort Light Pulses," Phys. Rev. Lett. **96**, 193901 (2006).
15. D. Faccio, A. Matijosius, A. Dubietis, R. Piskarkas, A. Varanavicius, E. Gaižauskas, A. Piskarkas, A. Couairon and P. Di Trapani, "Near and Far-Field evolution of laser pulse filaments in Kerr media," Phys. Rev. E **72** 037601 (2005)
16. D. Faccio, P. Di Trapani, S. Minardi, A. Bramati, F. Bragheri, C. Liberale, V. Degiorgio, A. Dubietis, A. Matijosius, "Far-field spectral characterization of conical emission and filamentation in Kerr media," J. Opt. Soc. Am. B **22**, 862–869 (2005).
17. M. Kolesik, E.M. Wright, and J.V. Moloney, "Interpretation of the spectrally resolved far field of femtosecond pulses propagating in bulk nonlinear dispersive media," Opt. Express **13**, 10729–10741 (2005).
18. G.G. Luther, A.C. Newell, J.V. Moloney, and E.M. Wright, "Short-pulse conical emission and spectral broadening in normally dispersive media," Opt. Lett. **19**, 789–791 (1994)
19. D. Faccio, A. Averchi, A. Couairon, A. Dubietis, R. Piskarskas, A. Matijosius, F. Bragheri, M.A. Porras, A. Piskarskas, and P. Di Trapani, "Competition between phase-matching and stationarity in Kerr-driven optical pulse filamentation," Phys. Rev. E **74**, 047603 (2006)
20. M. Kolesik, G. Katona, J.V. Moloney, and E.M. Wright, "Physical factors limiting the spectral extent and band gap dependence of supercontinuum generation," Phys. Rev. Lett. **91**, 043905 (2003)
21. E.R. Peck and K. Reeder, "Dispersion of air," J. Opt. Soc. Am. **62**, 958—962 (1972)
22. A. Couairon, E. Gaižauskas, D. Faccio, A. Dubietis and P. Di Trapani, Nonlinear X-wave formation by femtosecond filamentation in Kerr media, Phys. Rev. E **73**, 016608 (2006).
23. D. Faccio, A. Averchi, A. Couairon, M. Kolesik, J.V. Moloney, A. Dubietis, G. Tamosauskas, P. Polesana, A. Piskarskas, P. Di Trapani, "Spatio-temporal reshaping and X Wave dynamics in optical filaments," Opt. Express **15**, 13079–13095 (2007)
24. S. Champeaux and L. Bergé, "Postionization regimes of femtosecond laser pulses self-channeling in air," Phys. Rev. E **71**, 046604 (2005)
25. F. Courvoisier, V. Boutou, J. Kasparian, E. Salmon, G. Mejèan, J. Yu, and. J.P. Wolf, "Light filaments transmitted through clouds," Appl. Phys. Lett. **83**, 213–215 (2003)
26. M. Kolesik and J.V. Moloney, "Self-healing femtosecond light filaments," Opt. Lett. **29**, 590–592 (2004)

Understanding the physics that underly ultrashort laser pulse filamentation is a challenging task that must account for the many phenomena that are characteristic of filaments in all transparent media such as continuum generation, colored conical emission, pulse splitting and the formation of a high-intensity and strongly sub-diffractive core, i.e. a central peak whose width spreads at a slower rate compared to that of a Gaussian pulse [1]. This understanding is of paramount importance for applications, in particular in gases, such as nonlinear frequency conversion [2] , pulse compression [3] or plasma string generation [4].The formation of long range filaments in air was reported for the first time by Braun et al. [5], and explained as due to the Kerr-induced self-focusing which dominates over diffraction at sufficiently large input pulse powers. During the beam collapse high intensities are reached leading to ionization of the medium. Plasma-induced defocusing was proposed as a key player in the modeling of filamentation as a self-channeled light pulse or as a competition between nonlinear effects [6]. This understanding paved the way for many applications that rely on the formation of plasma strings within the filament such as induced lightning discharge [7, 8, 9] or efficient THz generation [10]. However, sub-diffractive propagation of intense light without significant ionization was also observed [11, 12].

Filamentation in condensed media has been explained as a spontaneous formation and interaction of nonlinear X Waves [13]. X Waves are stationary solutions to the paraxial propagation equation that, in a finite energy realization, may propagate without dispersion and without diffraction over long distances and exhibit a conical energy flux with "X" shaped intensity tails in both the near field (r,t) and far-field (θ,λ). Filamentation in air is associated to strong plasma generation and defocusing in a highly dynamical environment so that the presence of

#89996 - $15.00 USD Received 21 Nov 2007; revised 14 Jan 2008; accepted 16 Jan 2008; published 22 Jan 2008

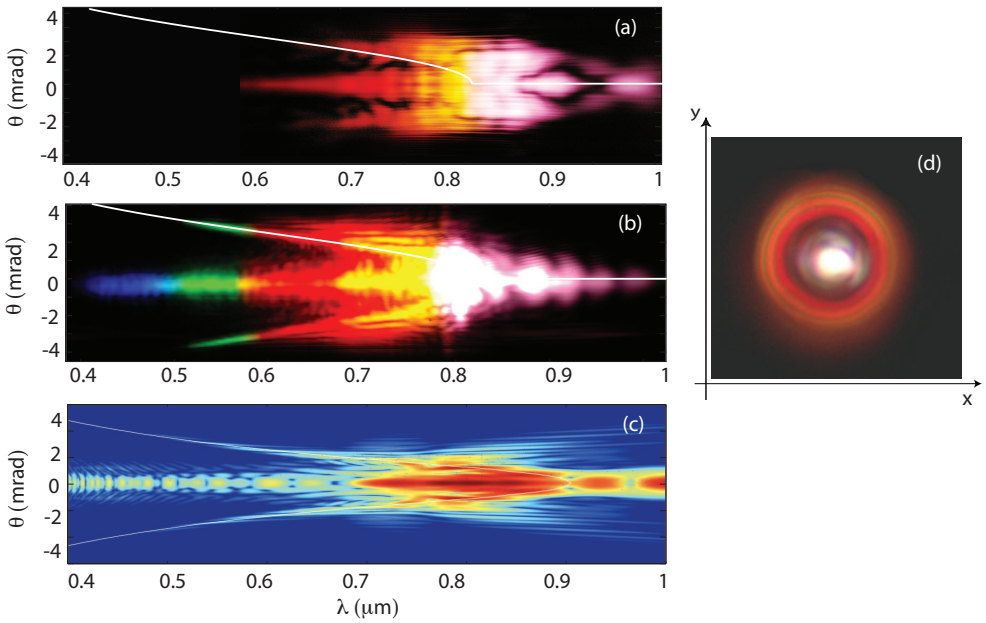

Fig. 1. Measured (θ,λ) spectra of filaments in air generated using a 2 m lens (a) and of a 10 m lens (b). (c) shows the numerically calculated spectrum for the experimental settings of (b). The white lines in all graphs show the best fits obtained with the X Wave relation Eq. (1). The filament appears as a white spot surrounded by colored rings when viewed on piece of paper a few meters after the end of the self-induced plasma string (d).

X waves that may still be considered as attractors for the pulse dynamics is far from obvious. Moreover, the energy flux established by the filamentation dynamics has never been previously shown to correspond to that of an X-wave. Here we show evidence that filaments in air may be interpreted as spontaneously generated X Waves, our results also establish that the subdiffractive propagation observed in the absence of plasma is sustained by an X-shaped conical energy flux refilling the intense core.

Numerical simulations shown in this work were carried using a modified Nonlinear Schrödinger equation for the pulse envelope $\mathscr{E}_{\omega,r,z} = \mathscr{F}(\mathscr{E}_{t,r,z})$, where $\mathscr{F}$ denotes Fourier transform, the derivation and details of which are recalled in Ref.s [1, 22]. All pulse parameters were chosen to match the experimental conditions described below and material parameters were chosen as described in Ref.[1]. Here we limit our description of the model by simply stating that we account for the full material dispersion, Kerr and delayed-Kerr (Raman) nonlinear response, plasma (generated by multiphoton and avalanche ionization) absorption and plasma defocusing described in the framework of a Drude model for inverse Bremsstrahlung processes, as well as the effect of nonlinear losses.

The experiments were carried out using 35 fs pulses centered at 800 nm with energy continuously tunable up to 40 mJ and 50 Hz repetition rate. The laser pulses were generated by an amplified Ti:Sapph system. Pulse duration and shape may be accurately controlled by an acousto-optic spectral shaper (Dazzler) inserted between the seed oscillator and the amplifier. Filamentation was observed without the need to focus the pulse although lenses with focal lengths up to 10 m were used in order to access the filamentation regime within the limited laboratory space. It is important to note that in the near-field (r,t) interference between the central spatio-temporal structure and the surrounding reservoir may impede any clear interpretation of

#89996 - $15.00 USD Received 21 Nov 2007; revised 14 Jan 2008; accepted 16 Jan 2008; published 22 Jan 2008

the underlying physics [15]. On the other hand it has been pointed out that the far-field (θ,λ) spectrum is the ideal space for observation of overall weakly localized wvepackets [16, 17]: the large reservoir reduces to peak centered at $\theta = 0$ while the tightly focused (in the near-field) space-time structure is now spread over a large area and is thus clearly visible. The far-field (θ,λ) spectra were measured with a commercial 1:1 imaging spectrometer (Andor Technologies) coupled to a modified color digital Nikon D70 camera with extended sensitivity from 400 nm to 1100 nm. Spectra were typically recorded with integration over ~ 50 laser shots. In Fig. 1(d) we show the filament obtained after a 10 m focal length lens with 4 mJ input energy, as viewed on a piece of paper a few meters after its end. A bright white-light central spot can be clearly seen surrounded by concentric colored rings, i.e. colored conical emission (CE). In Figs.1(a) and (b) we show the (θ,λ) spectra for filaments obtained with 2 m and 10 m focal length lens and $\sim$3 mJ input energy. The relative filament lengths were estimated to be roughly 1 m and 3 m, respectively. The CE starts to form only after the first $\sim$ meter and then gradually becomes visible as tails that extend toward blue-shifted wavelengths that are well separated from the axial supercontinuum (the central white spot in Fig. 1(d)). For comparison colored conical emission becomes clearly visible in condensed media after the first few mm of the filament. However in gases the nonlinear Kerr coefficient, responsible for the pulse reshaping, is roughly 1000 times smaller so that we should expect the conical emission to become clearly visible only after a few meters as indeed observed experimentally. Fig. 1(c) shows the numerically simulated intensity spectrum plotted over 5 decades, with the input conditions of Fig. 1(b) and shows a good quantitative agreement with the experiment. We note that while CE has been explained as the result of a phase-matched Four Wave Mixing (FWM) process [18], closer examination shows that this cannot explain any observed asymmetries [19]. Conversely the CE tails may be closely fitted using a three-wave mixing phase matching relation [20] or, equivalently, an analytical relation that describes the loci of the X Wave maximum intensity in the far-field [14, 23]:

$$k_\perp = \sqrt{k^2 - k_z^2} \quad \text{with} \quad k_z = k_0 + \Omega/v_g, \tag{1}$$

where $k_\perp$ is the transverse wave-vector, $k = \omega n(\omega)/c$, $k_0 = k = \omega_0 n(\omega_0)/c$ is the wave-vector at the pump ω_0, $\Omega = \omega - \omega_0$ and v_g is the group velocity of the X Wave pulse associated to the conical emission. The white solid lines in Figs.1(a)-(c) show the best fits obtained with Eq.(1) using the dispersion relation $n(\omega)$ for air [21] and confirm the remarkable precision with which this model is able to reproduce the conical emission features which may therefore be understood as a clear indication of X Wave formation the group velocity of which is determined by the fit. Notwithstanding the aforementioned technical difficulties in characterizing the filament near-field we may look for simpler evidence of X Wave formation e.g. by characterizing the beam spatial width evolution along the propagation direction. The solid line in Fig. 2(a) shows the numerically simulated Full Width at Half Maximum (FWHM) of the filament in the same conditions as in Fig. 1(c). The colored contour map shows the calculated plasma density in logarithmic scale. The plasma channel reaches a maximum electron density slightly higher than 10^{16} cm^{-3} and is maintained over a distance of roughly 2.5 m. The filament length is often defined as the length of the associated plasma channel: within this understanding the filament ends at a distance of $\sim$ 8.5 m. However we clearly observe that an intense spike continues to exist even after the end of the plasma channel and continues propagation without diffraction for another 1.5 m. This behavior is well reproduced by experimental measurements of the pulse FWHM (solid circles) obtained using photographic paper. Clearly in this region the subdiffractive propagation cannot be explained as a balance between Kerr self-focusing and plasma defocusing. It has been noted that GVD is an essential ingredient for the observation of self-guiding in the absence of ionization in air [24]. This is also a well-known characteristic of filamentation in condensed media that has been explained as due to the spontaneous formation of X Waves

#89996 - $15.00 USD Received 21 Nov 2007; revised 14 Jan 2008; accepted 16 Jan 2008; published 22 Jan 2008

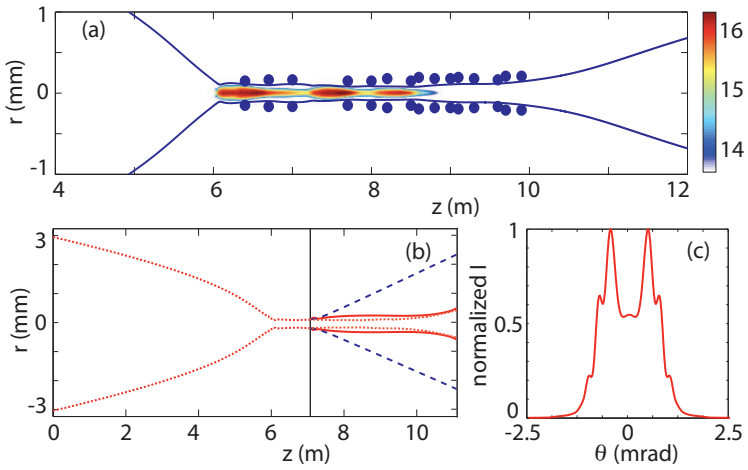

Fig. 2. (a) The solid lines shows the calculated FWHM of the filament generated with a 10 m focal length lens. The circles show the same quantity as measured experimentally while the contour plot represents the calculated plasma density in 1/cm^3 within the filament. (b) shows the calculated FWHM evolution of the filament when, at a distance of z=7 m, all nonlinear effects are switched off. The blue-dashed line indicates the expected FWHM of a linearly diffracting beam. Sub-diffractive propagation is observed in this linear regime over a 4 m distance (red solid line). The spatial far-field spectrum shows two peaks, a distinct feature of conical propagation (c).

[13]. Sub-diffractive propagation with negligible ionization and the important role of GVD in air both find a simple explanation if we interpret the central spike as the central peak of one or more non-diffracting X Waves. This means that a balance between chromatic dispersion and diffraction actually prevails in sustaining the subdiffractive propagation of the filament core. Indeed the intrinsic angular dispersion (different frequencies propagating at different angles) of X Waves is such that dispersion and diffraction compensate each other: removing one or the other will result in a diffracting peak. A further validation of this idea comes from Fig. 2(b): here we have taken the same numerical simulation in Fig. 2(a) (dotted line) and we have switched off all nonlinear effects at a distance $z = 7$ m, indicated by a solid line. Immediately after this point the linearly propagating peak FWHM increases by a factor ~ 1.5 corresponding to the sudden removal of self-focusing effects (red solid line). However the successive 4 m of propagation are characterized by strongly sub-diffractive propagation as is clearly seen by comparison with the expected linear diffraction of a Gaussian pulse with the same FWHM at z = 7 m (blue dashed line). We note that the sub-diffractive distances in the linear (solid line) and nonlinear simulations (dotted line) are similar and for distances greater than 10 m the FWHM profiles in the two cases actually overlap. Finally Fig. 2(c) shows the spatial far-field pattern of the "linear" filament where the two peaks (i.e. a ring in the full transverse space) outline the conical nature of the pulse confirming that the filament may be understood as a spontaneous formation of conical pulses or, more specifically, X Waves. This two peaked structure starts to form straight after the nonlinear focus and persists over the whole filament length, although the visibility depends strongly on the intensity of the on-axis super-continuum.

Finally, we consider the near-field transverse energy flux within the filament. This is advantageous as the linearly propagating reservoir has a rather low energy flux in the transverse direction which, on the contrary, is extremely lively in the nonlinear central portion

#89996 - $15.00 USD Received 21 Nov 2007; revised 14 Jan 2008; accepted 16 Jan 2008; published 22 Jan 2008

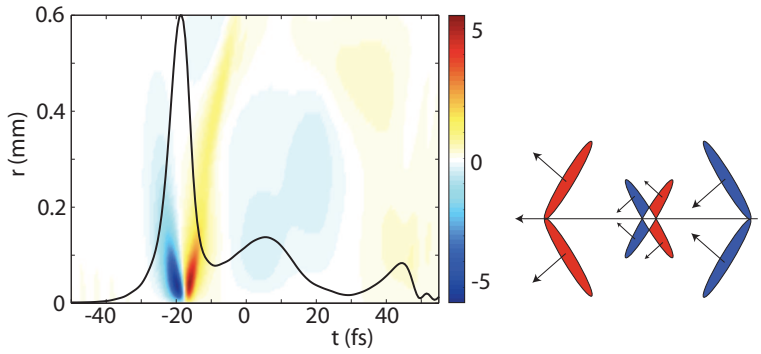

Fig. 3. Calculated transverse energy flux (in arbitrary units) for the same filament in Fig. 2(a) at a distance z = 7 m. The leading intensity peak clearly shows and X shaped profile the reflects the profile of the optical pulse. The leading X tail has an inward flux while the trailing tails has an outward flux. The diagram exemplifies this situation: plane waves propagating at an angle (i.e. along a cone) will give an X shaped energy flux in the region in which they overlap followed by an outgoing flux at the end of this region.

of the pulse. The energy flux in the transverse direction (radial) was obtained by monitoring $1/2i(\mathcal{E}^*\partial\mathcal{E}/\partial r - \mathcal{E}\partial\mathcal{E}^*/\partial r)$. A similar quantity may also be defined for the longitudinal flux by substituting the radial derivatives with temporal derivatives (data not shown). Figure 3 shows the calculated transverse energy flux for the filament at a distance $z = 7$ m. The black line shows the on-axis intensity profile of the pulse which is characterized by a strong leading peak followed by weaker oscillations. The leading peak is associated to a transverse energy flux that has a distinct X shape with the leading tails that are directed inwards and the trailing tails are directed outwards. This flux distribution is very different from that of a Gaussian pulse and the schematic diagram shows that it is exactly the flux to be expected from an ultrashort conical pulse where the X shape reflects the profile of the corresponding X Wave. The full movie shows that the X shaped conical flux forms shortly after the nonlinear focus and maintains a stationary profile over a long distance (until refocusing toward the pulse center occurs). The X-shaped conical flux confirms that in gases, as in condensed media, pulse reshaping is driven by the approach toward an X Wave. Finally, the conical flux also gives a simple explanation to the robustness of filaments in the presence of obscurants [25] and connects the surrounding photon bath to the central peak [26].

In conclusion we have shown that a number of features associated to ultrashort laser pulse filamentation in air such as CE, conical energy flux and sub-diffractive propagation in the absence of ionization or nonlinearities may be understood in terms of a spontaneous formation of X waves. Understanding that the filament pulse may be modeled as an X Wave would have an impact in many applications. For example the problem of creating longer and more stable plasma strings can be tackled by finding the X Wave or conical wave with minimized intensity fluctuations and longer sub-diffractive lengths while pulse compression may be optimized more effectively by flattening chirped phases in the spatial coordinate or in the full (r,t) domain rather than along the temporal coordinate.

The authors wish to acknowledge support from Access to Research Infrastructures activity in the Sixth Framework Programme of the EU (Contract No. RII3-CT-2003-506350, Laserlab Europe, Ultraviolet Laser Facility operating at the IESL-FORTH), PDT acknowledges support from the Marie Curie Chair project STELLA MEXC-CT-2005-025710 and ST acknowledges support from the Marie Curie Excellence Grant MULTIRAD MEXT-CT-2006-042683.

#89996 - $15.00 USD Received 21 Nov 2007; revised 14 Jan 2008; accepted 16 Jan 2008; published 22 Jan 2008